Journal of Alloys and Compounds 479 (2009) 342–347

Contents lists available at ScienceDirect

Journal of Alloys and Compounds

journal homepage: www.elsevier.com/locate/jallcom

Corrosion resistance and microstructure characterization of rare-earth-transition metal–aluminum–magnesium alloys

E.P. Banczek, L.M.C. Zarpelon, R.N. Faria, I. Costa *

Centro de Ciência e Tecnologia de Materiais, Instituto de Pesquisas Energéticas e Nucleares, IPEN-CNEN/SP, Av. Prof.Lineu Prestes, 2242, Cidade Universitária, 05508-900 São Paulo –SP, Brazil

ARTICLE INFO

Article history:
Received 5 September 2008
Received in revised form 12 December 2008
Accepted 15 December 2008
Available online 25 December 2008

Keywords:
Energy storage materials
Rare earth alloys and compounds
Corrosion
Scanning electron microscopy, SEM
Electrochemical impedance spectroscopy

ABSTRACT

This paper reports the results of investigation carried out to evaluate the corrosion resistance and microstructure of some cast alloys represented by the general formula: $La_{0.7-x}Pr_xMg_{0.3}Al_{0.3}Mn_{0.4}Co_{0.5}Ni_{3.8}$ (x = 0, 0.1, 0.3, 0.5, and 0.7). Scanning electron microscopy (SEM) and electrochemical methods, specifically, polarization curves and electrochemical impedance spectroscopy (EIS), have been employed in this study. The effects of Pr substitution on the composition of the various phases in the alloys and their corrosion resistance have been studied. The electrochemical results showed that the alloy without Pr and the one with total La substitution showed the highest corrosion resistance among the studied alloys. The corrosion resistance of the alloys decreased when Pr was present in the lowest concentrations (0.1 and 0.3), but for higher Pr concentrations (0.5 and 0.7), the corrosion resistance increased. Corrosion occurred preferentially in a Mg-rich phase.

1. Introduction

In recent years, nickel–metal hydride (Ni/MH) alloys for the negative electrode of a secondary battery have been incorporating many elements in addition to the basic composition of $LaNi_5$ with the purpose of improving the electrode performance [1–6]. In some cases, high hydrogen storage capacity, improved kinetics of hydrogen absorption and desorption, long cycle life, and good corrosion resistance have been achieved. Systematic studies to evaluate the cyclic stability of R–Mg–Ni type alloys (R: rare earth, Ca or Y) suggested a degradation mechanism composed of the following stages: pulverization of the alloy particles, oxidation/corrosion, and oxidation/passivation of the alloy active components [7,8]. The effect of the La–Mg–Ni–Co type alloys compositions on their microstructure, electrochemical properties, and hydrogen storage capacity has been thoroughly investigated by Liu et al. [9–14] and by Pan et al. [15–20]. Praseodymium has been incorporated into the alloys together with mish metal (MM) [21–30]. Pr content varying from 0 to 0.4 at.% in $MMAl_{0.3}Mn_{0.3}Co_{0.4}Ni_{4.0}$ alloys (MM = LaNdPr) has also been reported [31]. It has been shown that the electrochemical properties were greatly improved in an electrode alloy containing about 20 at.% Pr in the MM. Battery size cells in which the $(LaNdPr)Al_{0.3}Mn_{0.4}Co_{0.8}Ni_{3.5}$ electrode alloy contained about 17 at.% Pr in the MM showed a very long cycle life (1400 cycles) with reasonable rate capacity (1100 mAh when discharged at 5 C) [31]. In the annealed condition, the $La_{0.7}Mg_{0.3}Al_{0.2}Mn_{0.1}Co_{0.75}Ni_{2.45}$ alloy showed a maximum discharge capacity of 370.0 mAh/g [32]. The aim of this work is to investigate the influence of the substitution of La with Pr on the corrosion resistance of original $La_{0.7-x}Pr_xMg_{0.3}Al_{0.3}Mn_{0.4}Co_{0.5}Ni_{3.8}$ hydrogen storage alloys (x = 0, 0.1, 0.3, 0.5, and 0.7). The corrosion resistance of these alloys has been evaluated in the medium to which they are exposed inside the battery (6.0 M KOH solution) and in a more aggressive medium (0.6 M NaCl solution). Attempts have been made to correlate the corrosion behavior to the alloy microstructures.

2. Experimental

2.1. Microstructure and composition characterization

The alloys used in this investigation were prepared by Less Common Metals Ltd. (UK) in 5 kg batches melted in an induction heating furnace and cast in a water-cooled copper mold. The microstructures of these alloys were examined using a scanning electron microscopy (SEM) with energy dispersive X-ray (EDX) analysis facilities. The chemical compositions of these alloys, a general view of their as-cast microstructures, the X-ray diffraction (XRD) patterns, and a detailed phase analyses have all been reported in a previous paper [33]. In the present study, the surface of the specimens was also evaluated by SEM (+EDX) after polarization to investigate the presence of corrosive attack.

2.2. Corrosion resistance characterization

The corrosion resistance of the alloys was evaluated by electrochemical methods, specifically, electrochemical impedance spectroscopy (EIS) and potentiodynamic polarization curves (anodic and cathodic, separately). A three-electrode set-up cell

* Corresponding author. Tel.: +55 11 31339226; fax: +55 11 31339276.
E-mail address: icosta@ipen.br (I. Costa).

0925-8388/$ – see front matter © 2009 Elsevier B.V. All rights reserved.
doi:10.1016/j.jallcom.2008.12.075

was used in this study with a Pt wire and a mercurous oxide (Hg/HgO/6.0 M KOH) and (Ag/AgCl/KCl sat.) as the counter electrode (CE) and the reference electrodes (RE), respectively. The working electrode was prepared by cold epoxy resin mounting after electric contact was established with copper wire. The surface for exposure to the electrolyte was ground and polished to obtain a 1 μm finishing. The electrochemical behavior was evaluated with a Gamry frequency response analyzer (EIS 300) coupled to a potentiostat (PCI4/300).

The electrochemical tests were carried out in a 6.0 M KOH solution and in a 0.6 M NaCl solution, at 20 ± 2 °C. All the reagents used for the test solution preparation were per analytical (p.a.) grade. Firstly, samples of all the alloys were immersed in the 6.0 M KOH test solution, and the open circuit potential (OCP) was measured as a function of time. EIS tests were carried out after potential stabilization using perturbation voltage amplitude of ±10 mV, relative to the OCP, from 10 kHz to 10 mHz, with an acquisition rate of 10 points/decade. Immediately after the EIS tests, the OCP was measured to evaluate the potential stability. Subsequently, potentiodynamic polarization curves were obtained with a scanning rate of 30 mV/s. Attempts have been made to obtain polarization curves with slower scanning rates, but, due to the highly passive character of the alloys in the electrolyte used, only scattered data were obtained.

Based on the electrochemical results in the 6.0 M KOH solution, tests were carried out in a more aggressive medium for the alloys with a distinct corrosion behavior. Thus, the alloys without Pr and with 0.1 at.% Pr were selected for these tests, and the chosen medium was 0.6 M NaCl solution, which is a more corrosive electrolyte to ferrous alloys. Samples of these alloys were then polarized in 0.6 M NaCl solution using a scanning rate of 0.5 mV/s. The aim of this procedure was the evaluation of the alloys in a distinctly corrosive medium. To evaluate reproducibility, four specimens of each alloy were tested in this study.

3. Results and discussion

3.1. SEM and EDX characterization

The SEM images showing details of microstructure of the various alloys studied are shown in Fig. 1a–e. Phase analysis showed that the alloys are composed of a major or matrix phase (*M*), a gray phase (*G*), and a dark phase (*D*). A summary of the phases is given in Table 1 (a detailed analysis was performed by Zarpelon et al. [33]).

The *M* phase revealed a (La, Pr)/(Al, Mn, Co, Ni) atomic ratio of approximately 5, indicating it to be a 1:5 phase. Compared to the *D* phase, the *G* phase exhibited a higher Mg concentration (11 at.%).

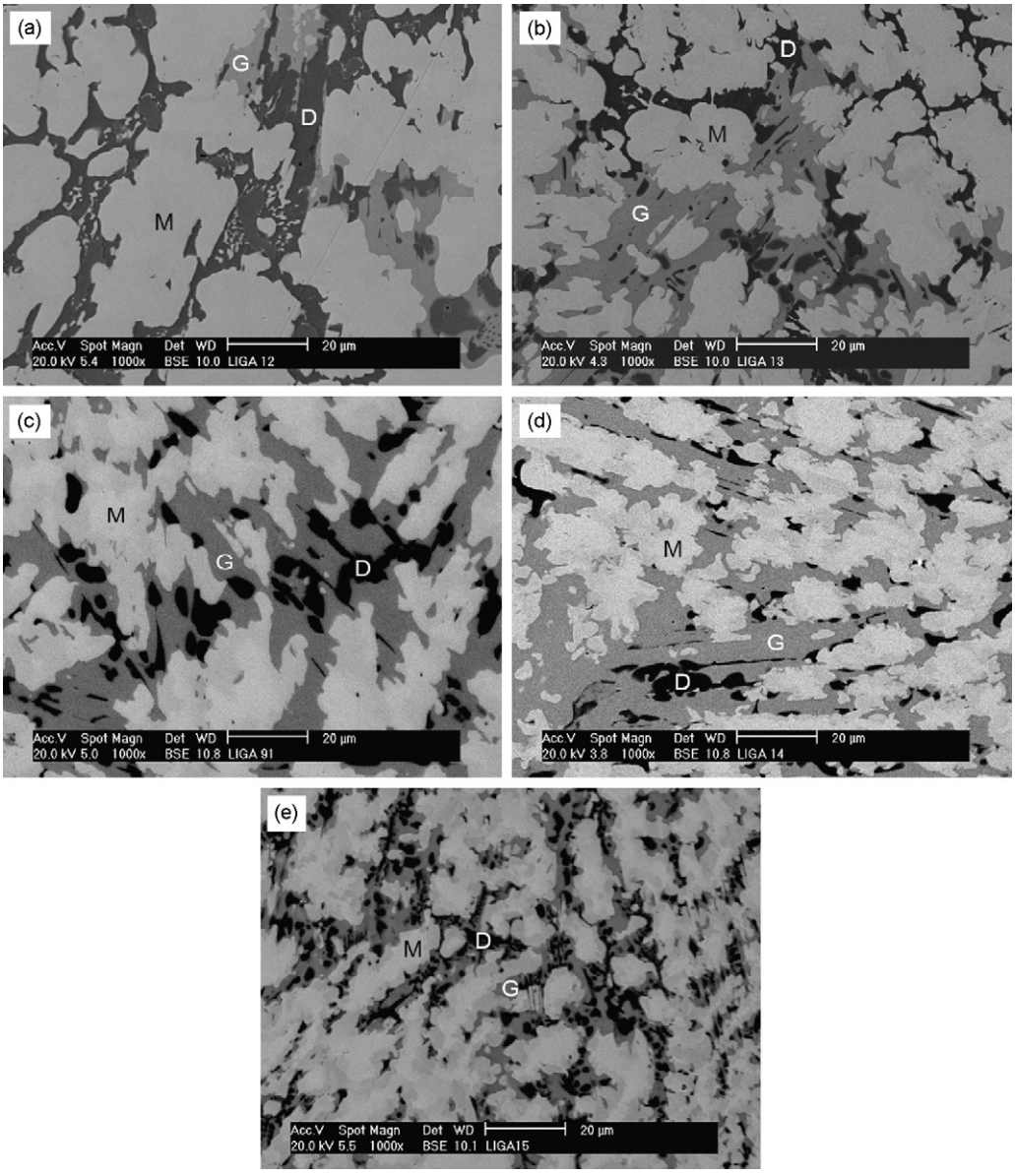

Fig. 1. SEM micrographs of the alloys investigated: (a) $La_{0.7}Mg_{0.3}Al_{0.3}Mn_{0.4}Co_{0.5}Ni_{3.8}$, (b) $La_{0.6}Pr_{0.1}Mg_{0.3}Al_{0.3}Mn_{0.4}Co_{0.5}Ni_{3.8}$, (c) $La_{0.4}Pr_{0.3}Mg_{0.3}Al_{0.3}Mn_{0.4}Co_{0.5}Ni_{3.8}$, (d) $La_{0.2}Pr_{0.5}Mg_{0.3}Al_{0.3}Mn_{0.4}Co_{0.5}Ni_{3.8}$ and, (e) $Pr_{0.7}Mg_{0.3}Al_{0.3}Mn_{0.4}Co_{0.5}Ni_{3.8}$.

Table 1
Composition determined by EDX at the centers of the matrix phase (*M*), the gray phase (*G*), and the dark phase (*D*) in the as-cast $La_{0.7-x}Pr_xMg_{0.3}Al_{0.3}Mn_{0.4}Co_{0.5}Ni_{3.8}$ alloys ($x = 0$ and 0.1).

Phase	Analyzed composition (at.%)						
	La	Pr	Mg	Al	Mn	Co	Ni
$x = 0$							
M	15.4 ± 0.6	–	<1	3.6 ± 0.3	3.6 ± 0.6	8.3 ± 0.5	68.4 ± 1.2
G	8.2 ± 0.3	–	10.9 ± 0.2	2.9 ± 0.4	9.5 ± 1.8	7.6 ± 0.1	60.9 ± 1.7
D	<1	–	1.8 ± 0.2	9.5 ± 0.4	15.1 ± 0.1	16.2 ± 0.3	56.8 ± 0.2
$x = 0.1$							
M	13.1 ± 0.3	2.5 ± 0.2	<1	4.2 ± 0.5	3.4 ± 0.8	8.2 ± 0.3	68.0 ± 0.1
G	7.3 ± 0.6	1.2 ± 0.2	11.5 ± 0.2	3.1 ± 0.3	8.8 ± 0.8	8.3 ± 0.3	59.8 ± 0.8
D	<1	<1	1.3 ± 0.1	9.6 ± 0.3	15.5 ± 0.1	16.7 ± 0.5	56.0 ± 0.5

The RE/Mg/(Al, Mn, Co, Ni) concentration in this phase obtained by EDX indicated an atomic ratio of about 1:2:9, corresponding to a possible $REMg_2Ni_9$ phase. The proportion of the dark phase diminished somewhat as the Pr-content was increased in the alloys. In the alloys with Pr contents above 0.3 at.%, this phase was smaller and more uniformly dispersed than on the alloys with 0.1 and 0.3 at.% Pr. In the other alloys, the dark phase apparently agglomerates in some areas of the alloy. The cause of this behavior is being investigated.

The dark phase contained Al, Mn, and Mg in significant amounts, and, hence, this phase might be more active compared to the matrix phase. A previous study of these alloys showed that the substitution of La with Pr in the LaMgAlMnCoNi-based alloys changed the grain structure from equiaxed to columnar [33].

3.2. Corrosion resistance characterization in 6.0 M KOH solution

3.2.1. Potentiodynamic polarization curves

Fig. 2 shows the (a) anodic and (b) cathodic potentiodynamic polarization curves obtained for the studied alloys. According to the polarization behavior obtained in 6.0 M KOH solution, the samples were arranged in two groups, Group 1 and Group 2. Most alloys showed very similar electrochemical behavior and very low corrosion current densities in a large potential range, typical of passive materials. However, two of the alloys, specifically, those with 0.1 and 0.3 at.% of Pr (Group 2), presented significantly higher corrosion currents than the others. Moreover, their corrosion potentials (OCP after stabilization) were much lower compared to the other alloys. Hydrogen bubbles were seen on most of the alloys during immersion for electrochemical test, suggesting the presence of phases with high overpotential for the hydrogen evolution reaction. Variations in the relative amount of these phases and, consequently, in the ratio of alloy surface coverage by hydrogen bubbles might have led to the differences found among the alloys. The dark phases and their distribution in the alloys might be the reason for this behavior. Furthermore, the presence of more active phases in the alloys might also contribute in lowering their corrosion potential. A current density increase occurred for the alloys associated with higher corrosion currents (Group 1) at potentials around 0.5. This could be associated to the evolution of the hydrogen bubbles from the alloy surface at this potential.

The cathodic polarization curves indicate a limiting current density (i_L) for the alloys with 0.0, 0.5, or 0.7 at.% Pr (Group 1), suggesting diffusion controlled corrosion process. This explains why in this group the alloy composition has no effect on their corrosion resistance. This could also be explained by the formation of a film precipitated on these alloy surfaces, leading to higher corrosion potentials and to diffusion controlled processes through the pores of this film. However, for the other alloys, there was no indication of a diffusion controlled process. Indeed, for the alloys with 0.1 and 0.3 at.% Pr (Group 2), the potential was dislocated to lower values, and the hydrogen reduction reaction seemed to be favored.

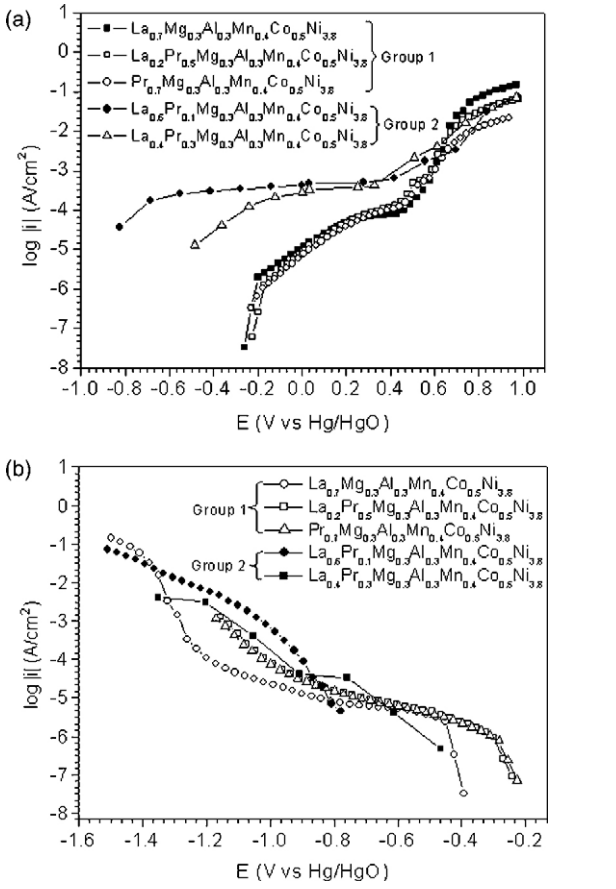

Fig. 2. Polarization curves of the $La_{0.7-x}Pr_xMg_{0.3}Al_{0.3}Mn_{0.4}Co_{0.5}Ni_{3.8}$ alloys ($x = 0$, 0.1, 0.3, 0.5, and 0.7) tested in 6.0 M KOH solution: (a) anodic polarization curves, and (b) cathodic polarization curves.

The polarization results in the KOH solution are supported by literature. Zhang et al. [34] found a passive behavior for the $La_{0.8}Mg_{0.2}Ni_{0.8}Mn_{0.1}Co_{0.5}Al_{0.1}$ alloy, and the current density values were very similar to those obtained in the present work. Furthermore, the corrosion potentials are similar to that of the alloys with 0.1 and 0.3 at.% Pr (Group 2).

3.2.2. SEM evaluation after polarization

Scanning electron microscopy was used to evaluate the characteristics of the alloy surfaces after polarization in 6.0 M KOH solution, fitting in each group (Group 1 and Group 2). The surfaces of the alloy without Pr ($La_{0.7}Mg_{0.3}Al_{0.3}Mn_{0.4}Co_{0.5}Ni_{3.8}$) and

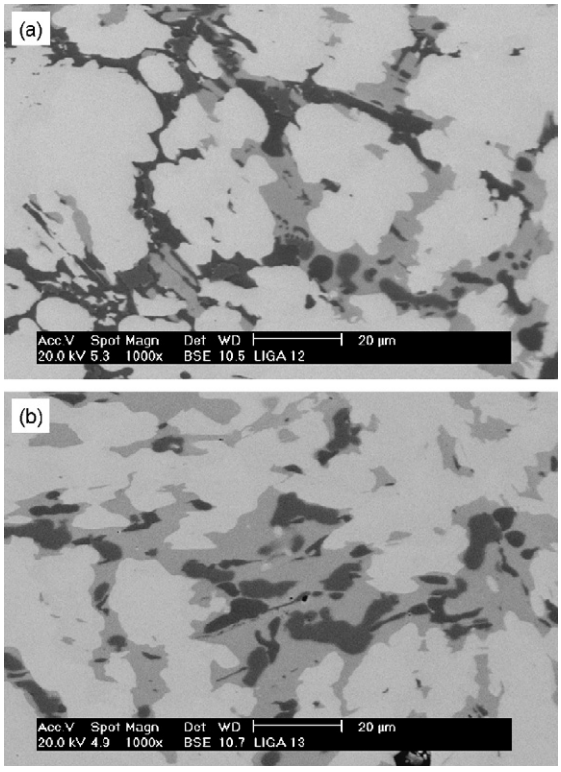

Fig. 3. SEM micrographs of the (a) $La_{0.7}Mg_{0.3}Al_{0.3}Mn_{0.4}Co_{0.5}Ni_{3.8}$ and (b) $La_{0.6}Pr_{0.1}Mg_{0.3}Al_{0.3}Mn_{0.4}Co_{0.5}Ni_{3.8}$ alloys after polarization in 6.0 M KOH solution.

the alloy with 0.1 at.% Pr ($La_{0.6}Pr_{0.1}Mg_{0.3}Al_{0.3}Mn_{0.4}Co_{0.5}Ni_{3.8}$) are shown in the micrographs of Fig. 3a and b, respectively. No indication of corrosion attack was found on either alloy surfaces. This result supports the passive behavior showed by the polarization curves.

3.2.3. Electrochemical impedance spectroscopy

The Nyquist and Bode phase angle diagrams for the various alloys studied are shown in Fig. 4a and b. Larger impedances were associated with the alloys of Group 1 (see insert in Fig. 4a). A large peak with high phase angles in the whole frequency range investigated was associated with the alloys in this group. However, two phase angle peaks were indicated by the alloys in Group 2 with much lower phase angles in the whole frequency range, suggesting less protective surface films on these alloys. Comparing the phase angles at higher frequencies associated with the alloys of Group 1, it can be seen that the peak moves into lower frequencies in the following order of Pr content in the alloy: 0.0, 0.5, and 0.7 at.%. It seems that the substitution of La with Pr leads to less protective passive films on the alloy surfaces mainly on those with 0.1 and 0.3 at.% Pr.

The results indicate a difference between the electrochemical behaviors of the studied alloys with higher corrosion current densities, where La was partially substituted by 0.1 and 0.3 at.% Pr. Despite that even for these two last alloys, the results suggest a fairly passive behavior, indicating that their corrosion resistance is not a limiting property for their use in the test solution used (6.0 M KOH solution).

3.3. Corrosion resistance characterization in 0.6 M NaCl solution

3.3.1. Potentiodynamic polarization curves

Fig. 5 shows the anodic polarization curves in 0.6 M NaCl solution of the alloy representative of Group 1 ($La_{0.7}Mg_{0.3}Al_{0.3}Mn_{0.4}$

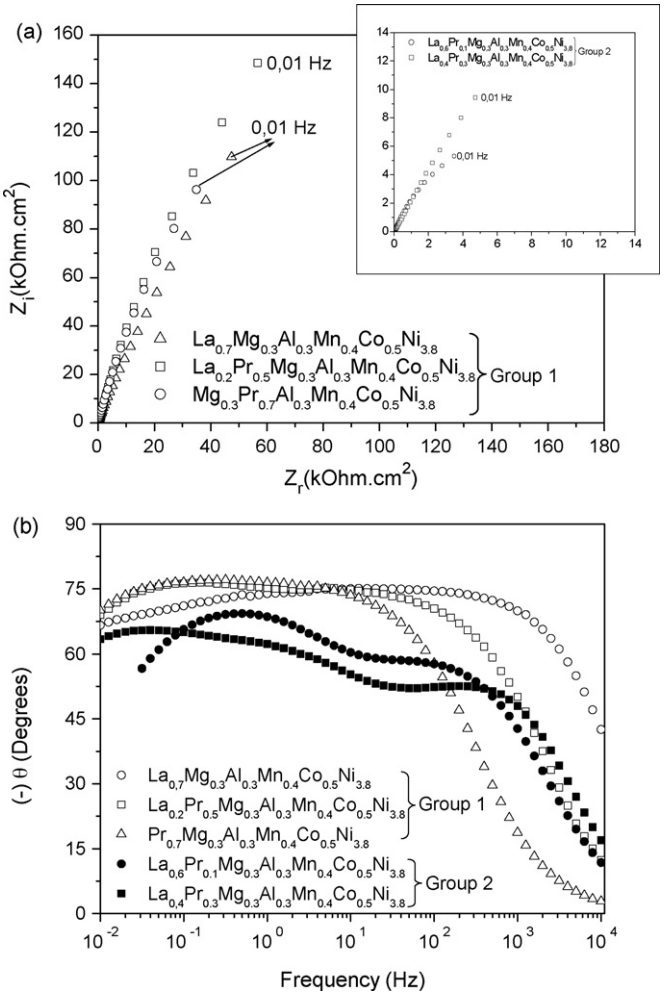

Fig. 4. Nyquist (a) and Bode phase angle (b) diagrams of the $La_{0.7-x}Pr_xMg_{0.3}Al_{0.3}Mn_{0.4}Co_{0.5}Ni_{3.8}$ alloys (x = 0, 0.1, 0.3, 0.5, and 0.7) tested in 6.0 M KOH solution.

$Co_{0.5}Ni_{3.8}$) and one of Group 2 ($La_{0.6}Pr_{0.1}Mg_{0.3}Al_{0.3}Mn_{0.4}Co_{0.5}Ni_{3.8}$). The polarization curves of both alloys did not show a typical passive behavior in the sodium chloride solution, even though the current densities at potential near to the corrosion potential were very low.

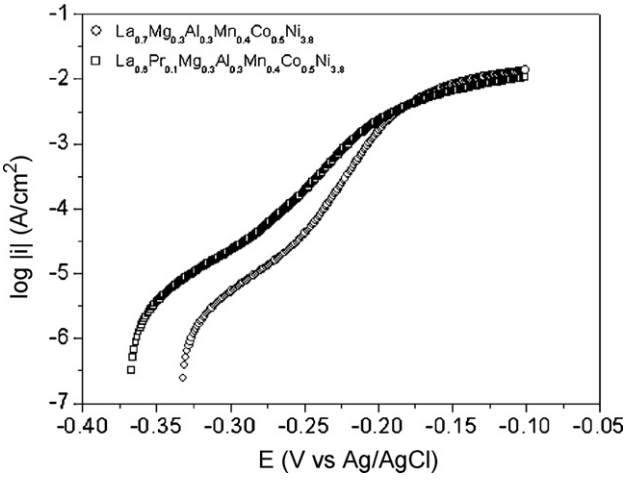

Fig. 5. Anodic polarization curves in 0.6 M NaCl solution for the $La_{0.7}Mg_{0.3}Al_{0.3}Mn_{0.4}Co_{0.5}Ni_{3.8}$ and $La_{0.6}Pr_{0.1}Mg_{0.3}Al_{0.3}Mn_{0.4}Co_{0.5}Ni_{3.8}$ alloys.

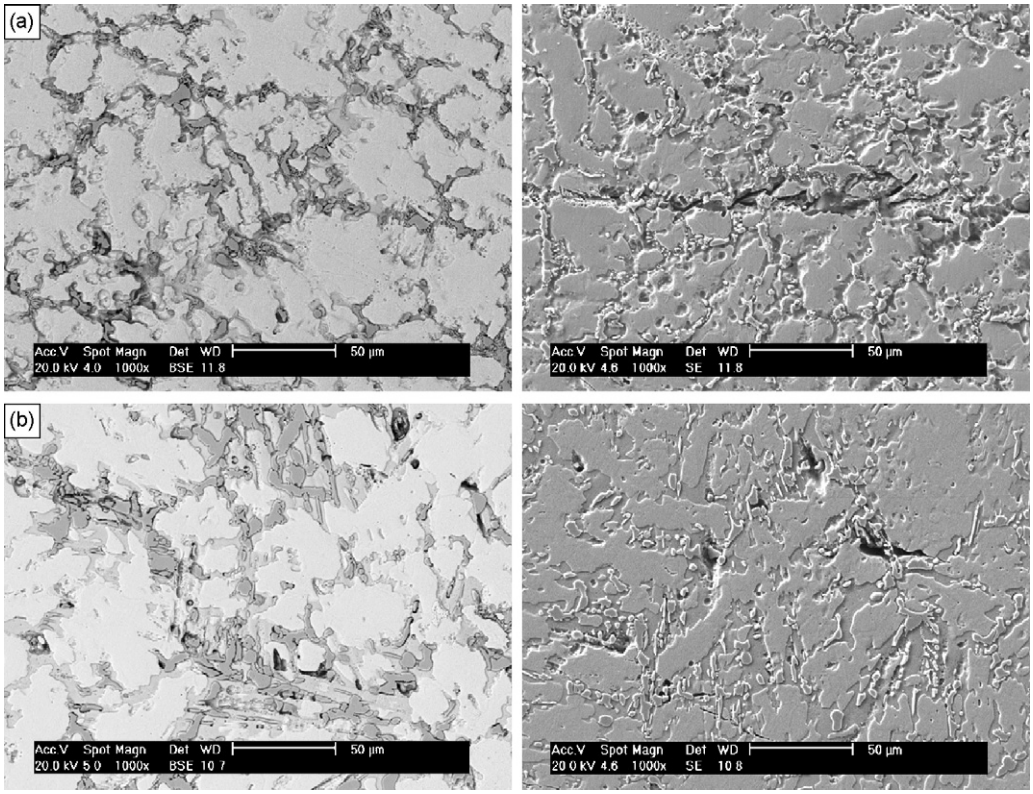

Fig. 6. Backscattered and secondary electron micrographs of the (a) $La_{0.7}Mg_{0.3}Al_{0.3}Mn_{0.4}Co_{0.5}Ni_{3.8}$ and (b) $La_{0.6}Pr_{0.1}Mg_{0.3}Al_{0.3}Mn_{0.4}Co_{0.5}Ni_{3.8}$ alloys after anodic polarization curves obtained in 0.6 M NaCl solution.

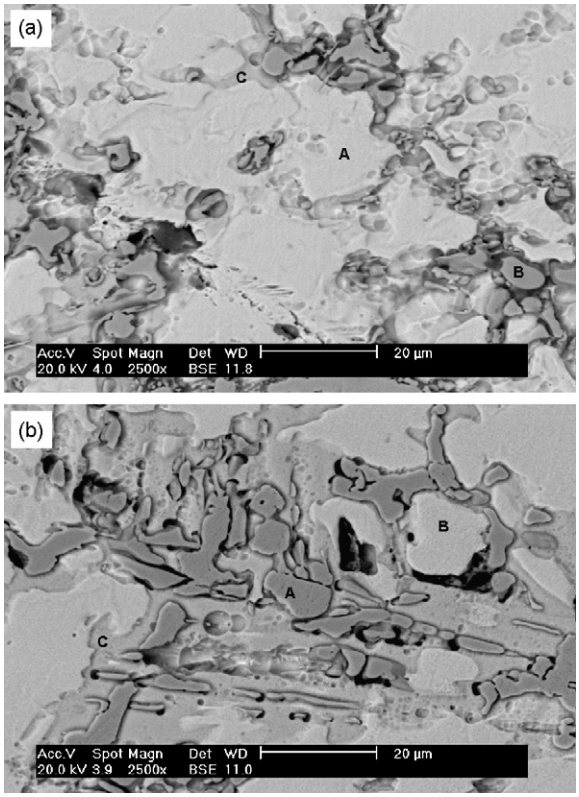

Fig. 7. Micrographs obtained by backscattered electrons image of the alloys (a) $La_{0.7}Mg_{0.3}Al_{0.3}Mn_{0.4}Co_{0.5}Ni_{3.8}$ and (b) $La_{0.6}Pr_{0.1}Mg_{0.3}Al_{0.3}Mn_{0.4}Co_{0.5}Ni_{3.8}$ after anodic polarization in 0.6 M NaCl solution. The regions on the micrographs indicated as A, B, and C were the areas analyzed by EDX.

The comparison of the polarization curves of both alloys, without and with 0.1 at.% Pr, indicates that the Pr addition decreased the corrosion resistance of the $La_{0.7}Mg_{0.3}Al_{0.3}Mn_{0.4}Co_{0.5}Ni_{3.8}$ alloy, leading to higher corrosion current densities and lower corrosion potential. These results suggest that Pr addition depolarized the anodic reaction. The results obtained support those obtained in the tested KOH medium. Similar results indicative of passive behavior were obtained by Meng et al. [35] for Pr-based amorphous alloys. The current density values at low overpotentials were similar to those of the present study.

3.3.2. SEM evaluation after polarization

SEM micrographs of the surfaces of $La_{0.7}Mg_{0.3}Al_{0.3}Mn_{0.4}Co_{0.5}Ni_{3.8}$ and $La_{0.6}Pr_{0.1}Mg_{0.3}Al_{0.3}Mn_{0.4}Co_{0.5}Ni_{3.8}$ samples anodically polarized in 0.6 M NaCl solution are shown in Fig. 6a and b, respectively. Areas of preferential corrosive attack can be seen on the polarized samples in 0.6 M NaCl solution, conversely from the observations on the 6.0 M KOH solution (Fig. 3).

It can be observed in detail in the backscattered electrons images shown in Fig. 7 that for the two polarized alloys, the gray phase was preferentially attacked (confirmed by EDX). This phase is rich in Mg, which explains the observed behavior. A comparison of Fig. 1a and b with Fig. 7 supports this indication. EDX analysis was carried out on three selected regions of the surface, indicated as A, B, and C, and the analyzed semiquantitative compositions are shown in Table 2. The chemical compositions of the analyzed regions allowed a correlation with the identified phased in the alloys, namely: region A (matrix phase, *M*), region B (dark phase, *D*), and region C (gray phase, *G*).

Table 2
Composition determined by EDX analysis on the anodically polarized $La_{0.7-x}Pr_xMg_{0.3}Al_{0.3}Mn_{0.4}Co_{0.5}Ni_{3.8}$ alloys. ($x = 0$ and 0.1) in 0.6 M NaCl solution.

Region	Analyzed composition (at.%)							Related phase
	La	Pr	Mg	Al	Mn	Co	Ni	
$x = 0$								
A	16.3 ± 0.3	–	<1	3.9 ± 0.1	1.6 ± 0.1	6.9 ± 0.1	71.1 ± 0.6	*M*
B	<1	–	1.6 ± 0.1	11.1 ± 0.1	14.9 ± 0.2	15.4 ± 0.2	56.6 ± 0.6	*D*
C	8.8 ± 0.2	–	12.8 ± 0.1	4.1 ± 0.1	7.8 ± 0.1	7.2 ± 0.1	59.3 ± 0.6	*G*
$x = 0.1$								
A	<1	<1	<1	10.3 ± 0.1	15.3 ± 0.2	16.5 ± 0.2	56.6 ± 0.6	*D*
B	13.3 ± 0.2	2.3 ± 0.1	1.4 ± 0.1	5.7 ± 0.1	3.6 ± 0.1	8.0 ± 0.1	66.0 ± 0.6	*M*
C	7.4 ± 0.2	1.6 ± 0.1	12.7 ± 0.1	3.3 ± 0.1	7.2 ± 0.1	7.9 ± 0.1	59.9 ± 0.6	*G*

4. Conclusions

The praseodymium content in the $La_{0.7-x}Pr_xMg_{0.3}Al_{0.3}Mn_{0.4}Co_{0.5}Ni_{3.8}$ alloys influenced their cast microstructures and corrosion resistance. It was found that the presence of a heterogeneous dark phase affected the hydrogen evolution cathodic reaction. The polarization curves showed that the alloys without Pr, and those with 0.5 or 0.7 at.%, were associated with improved corrosion performance comparatively to the other studied compositions. This was apparently related to the higher surface coverage of these alloys with hydrogen bubbles due to the higher hydrogen overvoltage on a particular phase in their microstructure. Although the electrochemical results showed differences in the corrosion resistance of the various alloys tested, the current densities associated were very low, even for those with higher corrosion currents. These results allow us to conclude that the corrosion resistance of the studied alloys is not a limiting property for their use as negative electrodes in Ni/hydride metal type batteries. The polarization results in a 0.6 M NaCl solution showed that it is more corrosive towards the investigated alloys than the 6.0 M KOH solution. A preferential attack of the Mg-rich phase occurred.

Acknowledgements

The authors wish to thank FAPESP and IPEN-CNEN/SP for the financial support and infrastructure made available to carry out this investigation. Thanks are also due to CNPq for the scholarship granted to E.P. Banczek.

References

[1] F. Feng, M. Geng, D.O. Northwood, Int. J. Hydrogen Energy 26 (2001) 725–734.
[2] H. Ye, Y.X. Huang, T.S. Huang, H. Zhang, J. Alloys Compd. 330–332 (2002) 866–870.
[3] M. Jurczyk, L. Smardz, K. Smardz, M. Nowak, E. Jankowska, J. Solid State Chem. 171 (2003) 30–37.
[4] Y. Liu, H. Pan, M. Gao, Y. Zhu, Y. Lei, Q. Wang, Int. J. Hydrogen Energy 29 (2004) 297–305.
[5] X. Zhang, D. Sun, W. Yin, Y. Chai, M. Zhao, Eur. J. Inorg. Chem. 11 (2005) 2235–2241.
[6] M.V. Ananth, M. Raju, K. Manimaran, G. Balachandran, L.M. Nair, J. Power Sources 167 (2007) 228–233.
[7] Y. Liu, H. Pan, M. Gao, Y. Lei, Q. Wang, J. Electrochem. Soc. 152 (2005) A1089–A1095.
[8] Y. Liu, H. Pan, M. Gao, Y. Lei, Q. Wang, J. Alloys Compd. 403 (2005) 296–304.
[9] Y. Liu, H. Pan, M. Gao, Y. Zhu, Y. Lei, J. Alloys Compd. 365 (2004) 246–252.
[10] Y. Liu, H. Pan, M. Gao, R. Li, Y. Lei, J. Alloys Compd. 376 (2004) 296–303.
[11] Y. Liu, H. Pan, M. Gao, R. Li, Y. Lei, J. Alloys Compd. 376 (2004) 304–313.
[12] Y. Liu, H. Pan, M. Gao, R. Li, X. Sun, Y. Lei, J. Alloys Compd. 387 (2005) 147–153.
[13] Y. Liu, H. Pan, M. Gao, R. Li, X. Sun, Y. Lei, J. Alloys Compd. 388 (2005) 109–117.
[14] Y. Liu, H. Pan, M. Gao, R. Li, Y. Lei, J. Alloys Compd. 389 (2005) 281–289.
[15] H. Pan, Y. Liu, M. Gao, Y. Zhu, Y. Lei, Q. Wang, J. Alloys Compd. 351 (2003) 228–234.
[16] H. Pan, Q. Jin, M. Gao, Y. Liu, R. Li, Y. Lei, J. Alloys Compd. 373 (2004) 237–245.
[17] H. Pan, Q. Jin, M. Gao, Y. Liu, R. Li, Y. Lei, Q. Wang, J. Alloys Compd. 376 (2004) 196–204.
[18] H. Pan, Y. Liu, M. Gao, Y. Zhu, Y. Lei, Q. Wang, J. Electrochem. Soc. 151 (2004) A374–A380.
[19] H. Pan, Y. Liu, M. Gao, Y. Lei, Q. Wang, J. Electrochem. Soc. 152 (2005) A326–A332.
[20] H. Pan, X. Wu, M. Gao, N. Chen, Y. Yue, Y. Lei, Int. J. Hydrogen Energy 31 (2006) 517–523.
[21] Y. Lei, J. Jiang, D. Sun, J. Wu, Q. Wang, J. Alloys Compd. 231 (1995) 553–557.
[22] C. Li, X. Wang, C. Wang, J. Power Sources 74 (1998) 62–67.
[23] M.N. Mungole, R. Balasubramaniam, K.N. Rai, Int. J. Hydrogen Energy 24 (1999) 467–471.
[24] I.P. Jain, M.I.S. Abu Dakka, Y.K. Vijay, Int. J. Hydrogen Energy 25 (2000) 663–667.
[25] W.X. Chen, Z.D. Xu, J.P. Tu, H.Y. Li, J. Yuan, S. Chen, S.N. Bao, Int. J. Hydrogen Energy 26 (2001) 675–681.
[26] D.B. Willey, D. Pederzolli, A.S. Pratt, J. Swift, A. Walton, I.R. Harris, J. Alloys Compd. 330–332 (2002) 806–809.
[27] Y. Chen, C.A.C. Sequeira, X. Song, R. Neto, Q. Wang, Int. J. Hydrogen Energy 27 (2002) 63–68.
[28] Z. Qingxue, J.M. Joubert, M. Latroche, D. Jun, A. Percheron Guegan, J. Alloys Compd. 360 (2003) 290–293.
[29] C.H. Peng, M. Zhu, J. Alloys Compd. 375 (2004) 324–329.
[30] Z. Zhang, S. Han, Y. Li, T. Jing, J. Alloys Compd. 431 (2007) 208–211.
[31] Z.H. Chen, M.Q. Lu, Y.L. Wang, Z.Q. Hu, J. Alloys Compd. 231 (1995) 550–552.
[32] H. Pan, N. Chen, M. Gao, R. Li, Y. Lei, Q. Wang, J. Alloys Compd. 397 (2005) 306–312.
[33] L.M.C. Zarpelon, E. Galego, H. Takiishi, R.N. Faria, Mater. Res. 11 (2008) 17–21.
[34] Y. Zhang, L. Jiao, H. Yuan, D. Song, Y. Wang, Y. Zhang, J. Alloys Compd. (2008), doi:10.1016/j.jallcom.2007.12.097.
[35] Q. Meng, J. Li, X. Bian, J. Alloys Compd. 424 (2006) 350–355.